

Article

TiO₂ Decorated Low-Molecular Chitosan a Microsized Adsorbent for a ⁶⁸Ge/⁶⁸Ga Generator System

Jun-Young Lee , Pyeong-Seok Choi, Seung-Dae Yang and Jeong-Hoon Park *

Korea Atomic Energy Research Institute, Jeongeup-Si 56212, Korea; lly01@kaeri.re.kr (J.-Y.L.); cps@kaeri.re.kr (P.-S.C.); sdyang@kaeri.re.kr (S.-D.Y.)

* Correspondence: parkjh@kaeri.re.kr; Tel.: +82-63-570-3571

Abstract: We report column material for a ⁶⁸Ge/⁶⁸Ga generator with acid resistance and excellent adsorption and desorption capacity of ⁶⁸Ge and ⁶⁸Ga, respectively. Despite being a core element of the ⁶⁸Ge/⁶⁸Ga generator system, research on this has been insufficient. Therefore, we synthesized a low molecular chitosan-based TiO₂ (LC-TiO₂) adsorbent via a physical trapping method as a durable ⁶⁸Ge/⁶⁸Ga generator column material. The adsorption/desorption studies exhibited a higher separation factor of ⁶⁸Ge/⁶⁸Ga in the concentration range of HCl examined (0.01 M to 1.0 M). The prepared LC-TiO₂ adsorbent showed acid resistance capabilities with >93% of ⁶⁸Ga elution yield and 1.6 × 10⁻⁴% of ⁶⁸Ge breakthrough. In particular, the labeling efficiency of DOTA and NOTA, by using the generator eluted ⁶⁸Ga, was quite encouraging and confirmed to be 99.65 and 99.69%, respectively. Accordingly, the resulting behavior of LC-TiO₂ towards ⁶⁸Ge/⁶⁸Ga adsorption/desorption capacity and stability with aqueous HCl exhibited a high potential for ion-exchange solid-phase extraction for the ⁶⁸Ge/⁶⁸Ga generator column material.

Keywords: ⁶⁸Ge/⁶⁸Ga generator; adsorbent; chitosan-TiO₂; acid resistance; ⁶⁸Ga-radiopharmaceuticals



Citation: Lee, J.-Y.; Choi, P.-S.; Yang, S.-D.; Park, J.-H. TiO₂ Decorated Low-Molecular Chitosan a Microsized Adsorbent for a ⁶⁸Ge/⁶⁸Ga Generator System.

Molecules **2021**, *26*, 3185. <https://doi.org/10.3390/molecules26113185>

Academic Editor: Peter J. H. Scott

Received: 27 April 2021

Accepted: 24 May 2021

Published: 26 May 2021

Publisher's Note: MDPI stays neutral with regard to jurisdictional claims in published maps and institutional affiliations.



Copyright: © 2021 by the authors. Licensee MDPI, Basel, Switzerland. This article is an open access article distributed under the terms and conditions of the Creative Commons Attribution (CC BY) license (<https://creativecommons.org/licenses/by/4.0/>).

1. Introduction

Gallium-68 (⁶⁸Ga) is a positron-emitting radionuclide obtained on-site using a ⁶⁸Ge/⁶⁸Ga generator without the need for an accelerator. ⁶⁸Ga has a short half-life (t_{1/2}; 67.71 min), decaying 89% through positron emission with a maximum energy of 1899.1 keV and a mean of 836.0 keV [1]. In human positron emission tomography/computed tomography (PET/CT), images reconstructed with PET spatial resolution phantom (⁶⁸Ga) have shown a resolution of 7.0 mm full width at half maximum (FWHM) [2], which is suitable for clinical-based scanning. Therefore, ⁶⁸Ga is a positron-emitting radionuclide that can be used equally with halogen radioisotopes (RIs) such as fluorine-18 and iodine-124. ⁶⁸Ga-based radiopharmaceuticals are increasingly being used in nuclear medicine worldwide for PET/CT tests [3,4]. Over the past few decades, clinical PET imaging research using ⁶⁸Ga has increased tremendously [5]. ⁶⁸Ga-radiopharmaceuticals have been recognized for the diagnosis of bone infection and tumors. For example, ⁶⁸Ga-labeled somatostatin receptor-specific peptides (SSTRs) [6], 1,4,7,10-tetra-azacyclododecane-1,4,7,10-tetraacetic acid-D-Phe¹-Tyr³-octreotide (DOTATOC) in the European Union and DOTA-Tyr³-octreotate (DOTATATE) in the United States, are being used successfully for PET imaging [7,8].

⁶⁸Ge/⁶⁸Ga generators are commercially available worldwide, and their use in the medical field is increasing rapidly [9]. Therefore, researching ⁶⁸Ge/⁶⁸Ga generator column materials and studying the capability of adsorption and desorption of ⁶⁸Ge and ⁶⁸Ga radionuclides represent an urgent scientific need of the involved community. Most column adsorbents acting as the core elements of the ⁶⁸Ge/⁶⁸Ga generator use metal oxides [10]. In general, metal oxides have good adsorption capacities for metal ions and provide high surface area with varying surface functional groups that can interact with heavy metal ions [11,12]. As a result, they show remarkable potential for the removal of heavy metal

ions. However, the metal oxide adsorbents are poor in acid-resistance [13]. A prefiltration process of eluted Ga-68 is performed to overcome this limitation. Different types of metal oxides have been intensively investigated for $^{68}\text{Ge}/^{68}\text{Ga}$ generator systems, such as SnO_2 , SiO_2 , TiO_2 , ZnO_2 and Al_2O_3 [14–16]. However, such adsorbents have low acidic stability and high ^{68}Ge breakthrough, which deteriorates over time.

Chitosan is a natural biopolymer obtained by the deacetylation of chitin. It is the main structural component of crustacean exoskeletons [17–19]. It is a biocompatible material and is harmless to the human body even when used as an inert support for adsorbents [20]. In particular, chitosan in the presence of amino and hydroxyl functional groups can react with metal ions by electrostatic forces and hydrogen bonds [20,21]. Furthermore, it is possible to increase the capacity of capturing metal ions by exerting a synergistic effect by titanium trapped on the chitosan polymeric matrix [17]. For the removal of heavy metal ions from wastewater, studies have been conducted based on chitosan-adsorbents. Still, as a material for adsorption/separation of RI generators, studies considering elution pressure, acid resistance, radiation resistance, and adsorption and desorption efficiency of RIs represent a new approach [22,23].

In a previous paper [24], we described the adsorption and desorption capacity of $^{68}\text{Ge}/^{68}\text{Ga}$ by synthesizing spherical chitosan- TiO_2 of 700 μm . Compared to these results, we expect to improve the adsorption and desorption capacity of $^{68}\text{Ge}/^{68}\text{Ga}$ and acid-resistance by adjusting the size of the chitosan- TiO_2 adsorbent using low molecular chitosan.

In this study, low molecular chitosan and titanium dioxide (P25) were used to develop $^{68}\text{Ge}/^{68}\text{Ga}$ generator column material to ensure the high adsorption/desorption capacity of ^{68}Ge (parent nuclide)/ ^{68}Ga (daughter nuclide), respectively, while maintaining its stability in hydrochloric acid, which is generally used as a ^{68}Ga eluent (Scheme 1).



Scheme 1. Scheme of a $^{68}\text{Ge}/^{68}\text{Ga}$ generator column system based on the chitosan- TiO_2 adsorbent.

2. Results

2.1. Preparation and Characterization of LC- TiO_2

Low molecular chitosan and titanium dioxide were used as an inert support and stationary phase to synthesize a microsized LC- TiO_2 adsorbent with excellent adsorption/desorption capability for $^{68}\text{Ge}/^{68}\text{Ga}$, while securing stability towards corrosive HCl.

The reaction of viscous acetic acid-based low molecular chitosan with titanium dioxide (P25) precursor formed a chitosan-titanium composite-based polymeric matrix. (Figure 1).

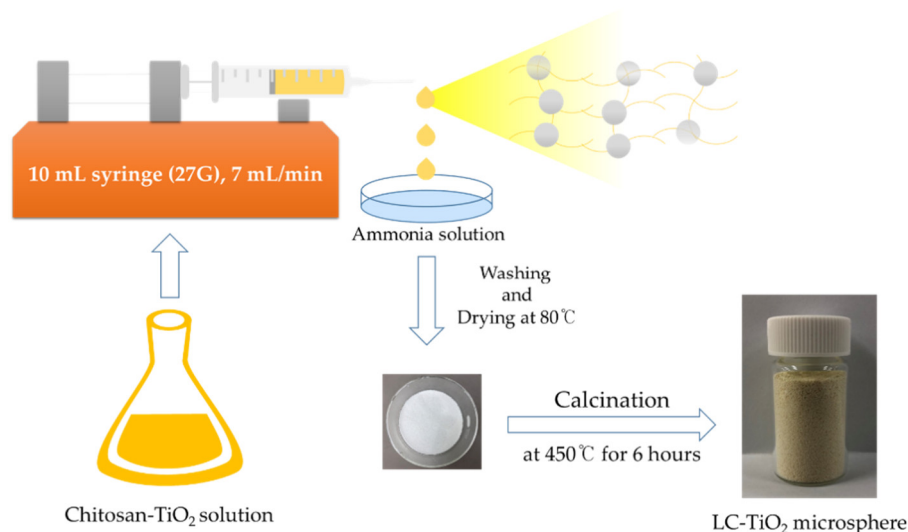


Figure 1. Synthesis procedure for low molecular chitosan-TiO₂ adsorbent via physical deposition method.

The synthesized LC-TiO₂ adsorbent was characterized for particle size, surface morphology and elementary composition with a scanning electron microscope-energy dispersive X-ray spectrometer (SEM-EDX) and elemental mapping system. SEM images of LC-TiO₂ adsorbent are shown in Figure 2. In Figure 2a, the average particle size of the synthesized LC-TiO₂ is around $250 \pm 30 \mu\text{m}$. At higher magnification (Figure 2b,c), the TiO₂ trapped chitosan polymer was confirmed, which was physically bonded in a polymeric structure. Besides, elemental mapping showed that titanium nanoparticles were evenly distributed in the LC-TiO₂.

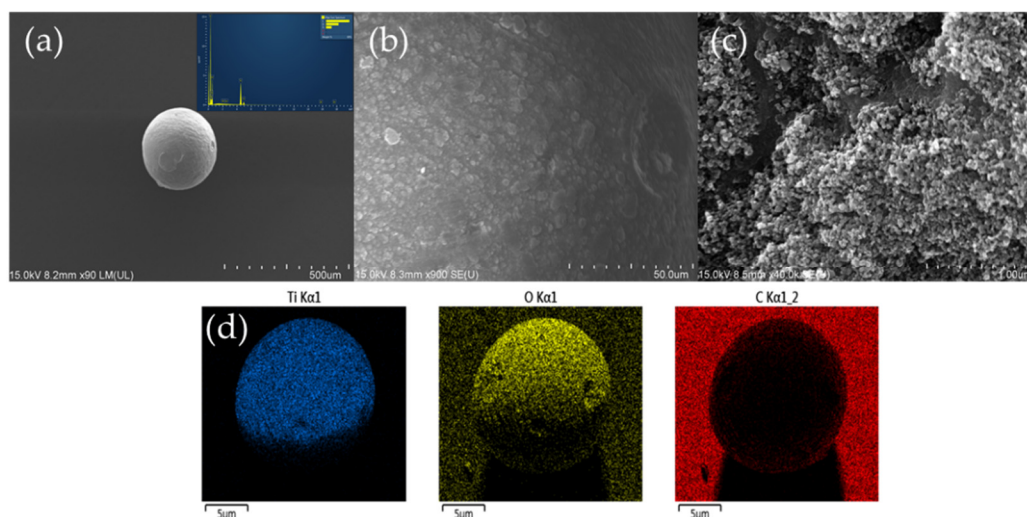


Figure 2. SEM images of LC-TiO₂ adsorbent (a) magnification 80 \times (b) magnification 1100 \times (c) magnification 50,000 \times and elements maps (d) magnification 70 \times (scale = 5 μm) from SEM-EDX.

Figure 3a shows the X-ray diffraction (XRD) pattern of LC-TiO₂ adsorbent prepared by a mechanical stirring method. The XRD peaks can be perfectly indexed to the anatase and rutile structures of TiO₂ (COD No. 9015929 and ICDD No. 01-088-1172, respectively).

The average crystallite size (\AA) of LC-TiO₂ adsorbent can be estimated according to the diffraction and reflection using the Williamson-Hall method. The crystallinity of anatase and rutile phases was confirmed, which has an individual crystal size of 167 and 653 \AA . The crystal phase and size were similar to P25, reflecting the physical sorption to the chitosan polymeric template without modification of P25 during synthesis.

The nitrogen adsorption-desorption (BET) isotherm (Figure 3b) of LC-TiO₂ adsorbent was measured. The pore size distribution plot was measured using the Barrett-Joyner-Halenda (BJH) method from the desorption branch of the isotherm. The physical properties were measured with a high surface area of $36.05 \text{ m}^2 \cdot \text{g}^{-1}$, pore-volume and pore size of $0.13 \text{ cm}^3 \cdot \text{g}^{-1}$ and 14.52 nm, respectively.

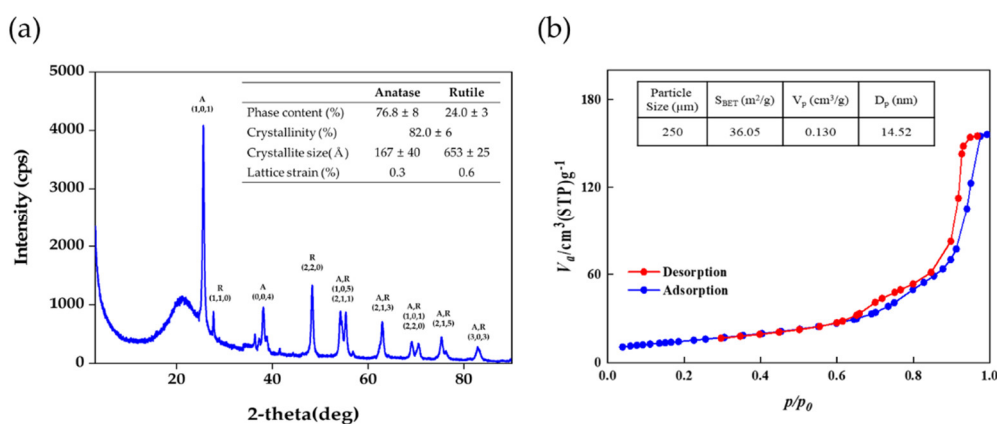


Figure 3. Characterization of LC-TiO₂ adsorbent with (a) X-ray diffraction pattern and (b) N₂ adsorption/desorption capacity.

2.2. Acid Resistance

Metallic impurities (Table 1) were measured after immersing LC-TiO₂ in 0.05 M HCl eluent. The concentration of titanium ion was confirmed to be 4 ppb. The level of titanium was too low, proving the mechanical stability of the synthesized composite. Considering the material stability and the half-life of ⁶⁸Ge (parent radionuclide) of ~271 days, the column material can be used as a ⁶⁸Ge/⁶⁸Ga generator for >1 year. Besides, the concentration of other metallic impurities such as Sc, V, Cr, Mn, Zn, Ru, Rh, Pd, Ag, and Cd were determined in immersed LC-TiO₂ with 0.05 M HCl and found to be at extremely low levels and always under $15 \text{ ng} \cdot \text{mL}^{-1}$ (ppb) as shown in Table 1.

Table 1. Measured metallic impurities in unit of ppb ($\text{ng} \cdot \text{mL}^{-1}$), in 0.05 M hydrochloric acid and blank, after incubation of the LC-TiO₂ adsorbent.

Elements	Measured Conc.	Blank Conc.
Sc	0.37 ± 0.016	0.43 ± 0.010
Ti	4.05 ± 0.004	0.13 ± 0.003
V	0.41 ± 0.008	0.42 ± 0.004
Cr	0.95 ± 0.040	0.92 ± 0.006
Mn	0.21 ± 0.001	0.15 ± 0.001
Zn	12.0 ± 0.041	4.82 ± 0.010
Ru	0.14 ± 0.001	0.14 ± 0.001
Rh	N.A.	N.A.
Pd	0.31 ± 0.001	0.33 ± 0.001
Ag	N.A.	N.A.
Cd	0.19 ± 0.000	0.19 ± 0.001

2.3. Distribution Coefficient

The distribution coefficient of $^{68}\text{Ge(IV)}/^{68}\text{Ga(III)}$ ions on the LC-TiO₂ adsorbent at different molarity of HCl are displayed in Figure 4. The K_d value of parent radionuclide $^{68}\text{Ge(IV)}$ was maximum at pH 2 while the $^{68}\text{Ga(III)}$ was less than $1 \text{ mL}\cdot\text{g}^{-1}$ at 0.05 M HCl. In theory, at concentrations lower than 0.01 M HCl, the K_d value should increase by hydrolysis of the Ga ion [25]. The Ga(III) ion changes from $\text{Ga}^{3+} \rightarrow \text{Ga(OH)}^{2+} \rightarrow \text{Ga(OH)}_2^+ \rightarrow \text{Ga(OH)}_3$ to Ga(OH)_4^- , which is expected for the reduced desorption capacity of the Ga (III) ion. In addition, $^{68}\text{Ge(IV)}$ was evaluated for having high adsorption capacity (K_d ; $3512 \pm 0.630 \text{ mL}\cdot\text{g}^{-1}$). The $^{68}\text{Ge}/^{68}\text{Ga}$ separation factor (SF) using metal oxide is about $\sim 10^2$. In particular, the SF for titanium dioxide is ~ 230 . In contrast, the adsorbent developed in this study showed that was more than 1000 time higher.

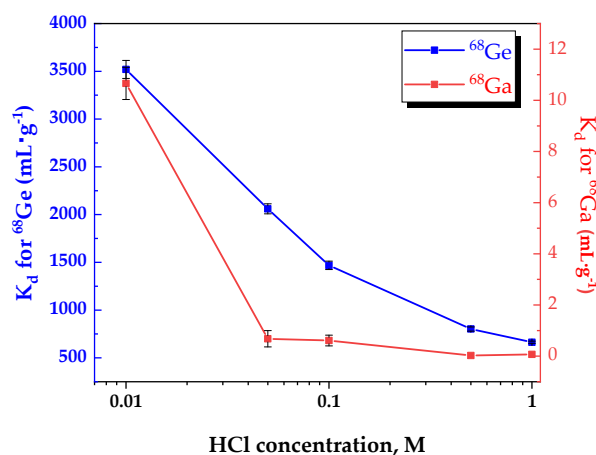


Figure 4. The distribution coefficient of ^{68}Ge and ^{68}Ga in various conc. HCl with LC-TiO₂.

2.4. Column Study

Evaluation of the adsorption capacity of ^{68}Ge depending on time is required for preparing the $^{68}\text{Ge}/^{68}\text{Ga}$ generator column material. The adsorption yield of ^{68}Ge reached the maximum capability within 3 h (Figure 5). The elution profile (Figure 6) of ^{68}Ga depended on the HCl concentration. $>93\%$ of the ^{68}Ga radioactivity was eluted with 0.05M HCl in the 1 mL volume due to the high separation factor of $^{68}\text{Ge}/^{68}\text{Ga}$. The breakthrough of ^{68}Ge was confirmed to be $1.6 \times 10^{-4}\%$. This result guarantees the quality of ^{68}Ga -radiopharmaceuticals.

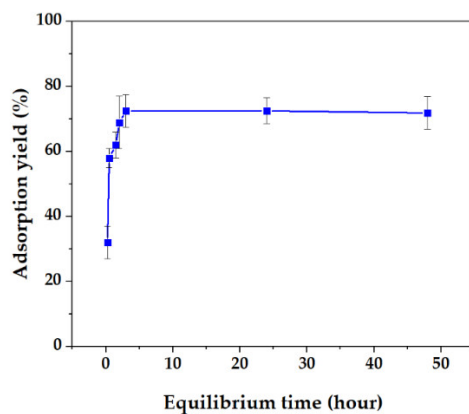


Figure 5. The adsorption capacity of ^{68}Ge depending on incubation time.

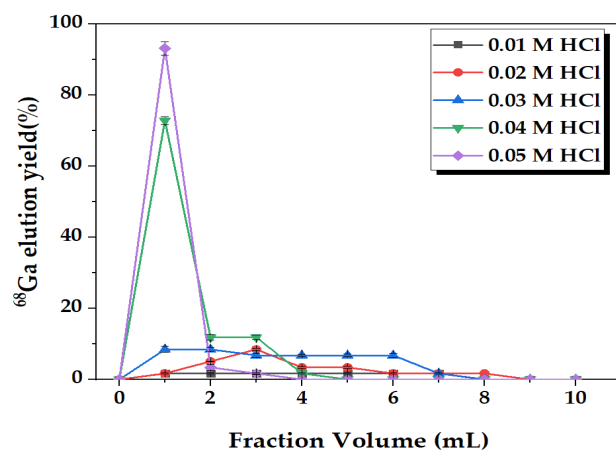


Figure 6. Elution profile of ^{68}Ga from LC-TiO₂ column.

2.5. Radiolabeling and In Vivo Evaluation

After the reaction, radiochemical yields% (RCY%) of ^{68}Ga -DOTA and ^{68}Ga -NOTA were 99.65% and 99.69%, respectively. Experimental data are supplied for each chelator in Figure 7a–c.

In vivo small-animal PET studies using ^{68}Ga -DOTA and ^{68}Ga -NOTA (Figure 7b) show the possibility of introducing ^{68}Ga eluted from the column into radiopharmaceuticals. Radiolabeled DOTA and NOTA chelators are potential candidates for the diagnosis of various diseases and cancer. Radiolabelled ^{68}Ga exhibited high accumulation in kidney and low uptake in normal tissues in a mouse model, as shown in Figure 7.

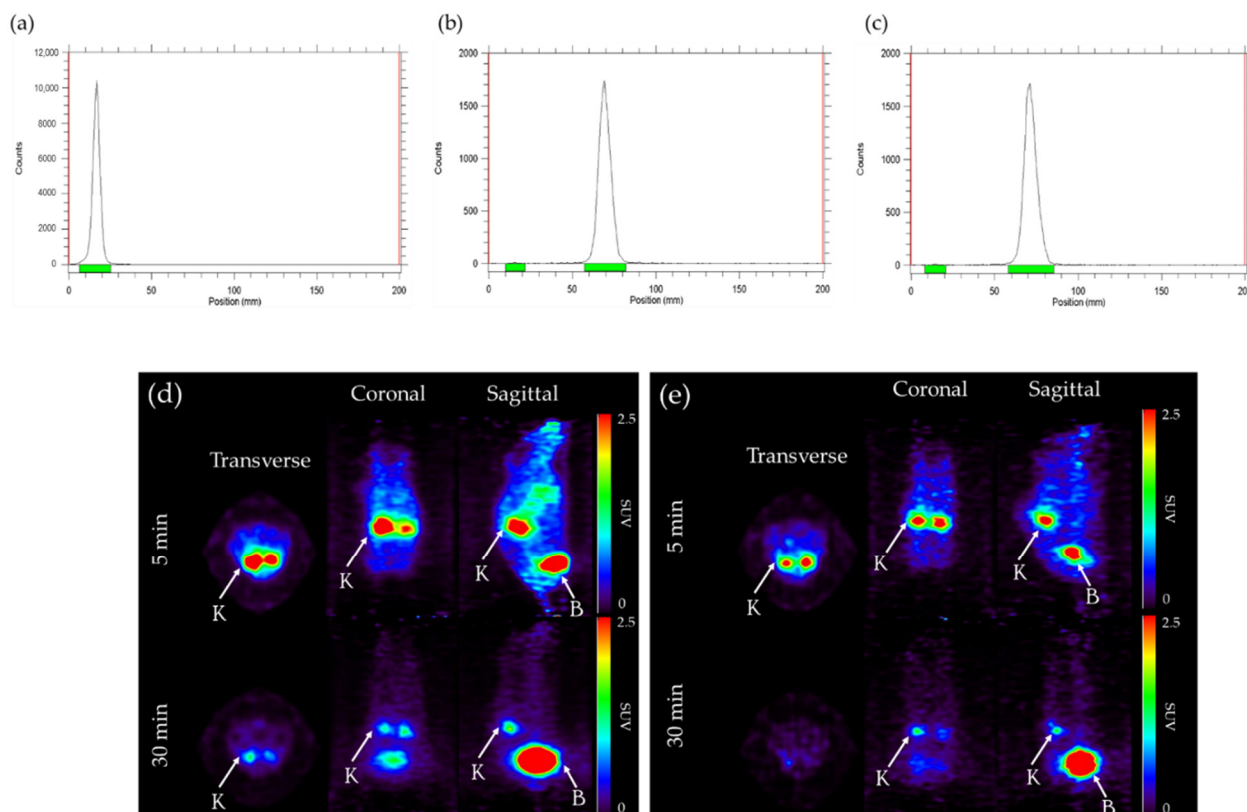


Figure 7. ^{68}Ga labeling study. Radio instant thin layer chromatography of (a) ^{68}Ga -chloride, (b) ^{68}Ga -DOTA, and (c) ^{68}Ga -NOTA on silica-gel papers developed in MeOH/10%NH₄OAc as a mobile phase under optimized conditions. Whole-body PET images of balb/c mice at 5 min and 30 min post injection of 1.1 MBq of (d) ^{68}Ga -DOTA and (e) ^{68}Ga -NOTA.

3. Discussion

The LC-TiO₂ adsorbent was synthesized by a physical deposition method. This method is effective in enhancing the trapping of titanium dioxide nanoparticles in the polymeric chitosan. The synthesized LC-TiO₂ was characterized by SEM, EDX, XRD and BET equipment.

The size and morphology of the adsorbent were confirmed through SEM analysis. LC-TiO₂ was synthesized to enhance the conditions (elution pressure, stability, adsorption/desorption capacity) necessary for its use as a column material for a ⁶⁸Ge/⁶⁸Ga generator system. Compared to the 700 μm sized chitosan-TiO₂ adsorbent in our previous study [24], spherical LC-TiO₂ of 250 μm was synthesized, which has low elution pressure and high reactivity between the eluent and the adsorbent. In the EDX and mapping element analysis results, it was speculated that TiO₂ could effectively react with ⁶⁸Ge and ⁶⁸Ga metal ions and confirming that Ti is evenly distributed in the chitosan template.

The TiO₂ used in this study was Degussa P25 of about 21 nm commercial size, with a mixture of about 80% anatase and 20% rutile in XRD measurements. After a physical trap reaction of low molecular chitosan and TiO₂, it was confirmed that the homozygous polymorphic form of anatase and rutile was maintained. Titanium tetraisopropoxide (TTIP) used as a Ti source other than P25 can be hydrolyzed and undergo a phase transition from an anatase phase to a rutile structure even at low temperatures by H⁺ generated as a by-product. It is known that the ratio of the rutile phase increases [26].

Figure 3b shows the N₂-sorption graph and pore distribution obtained through BET measurement of LC-TiO₂. The BET-specific surface area of the LC-TiO₂ adsorbent prepared by the physical trap method was measured to be 36.05 m²·g⁻¹. From the N₂-sorption graph in 3(b), it can be seen that pores of 14.52 nm exist due to the difference in the adsorption and desorption curves occurring at the point where the relative pressure is about 0.6.

In the acid resistance results, the content of metal impurities was measured using ICP-MS (inductively coupled plasma-mass spectrometer) equipment. Stability evaluation of the elution pressure of ⁶⁸Ga and hydrochloric acid as eluent was performed to determine whether it could be introduced as a column material for a ⁶⁸Ge/⁶⁸Ga generator. Since a low-molecular chitosan-Ti based adsorbent is used, stability in an acid solution against Ti metal ions must be secured. In general, Ti⁴⁺ ion can be derived from Ti metal using acid, during which there is a migration of H⁺ ions from the acid to the metal surface, forming H⁺ and H₂ [13]. The analysis of metal element content confirmed that background-level elements were included, and further studies are being conducted to secure long-term stability.

The distribution coefficient of ⁶⁸Ge and ⁶⁸Ga on LC-TiO₂ at different molarities of HCl is displayed in Figure 4. The adsorption capacity of ⁶⁸Ge was maximum at 0.01 M HCl, and the trend continued to decrease. The *K_d* value of ⁶⁸Ga is shown, which had a slight difference, and a similar level of high desorption ability above a concentration of 0.05 M HCl.

Considering the distribution coefficient results of ⁶⁸Ge and ⁶⁸Ga, a column study was performed using 0.05 M hydrochloric acid with a high SF value (SF⁶⁸Ge/⁶⁸Ga = 2984 ± 9.542).

The ⁶⁸Ge source was dispersed in 0.01 M HCl, and then adsorbed onto LC-TiO₂ adsorbent for 3 h in consideration of the previously evaluated adsorption/desorption capacity of ⁶⁸Ge/⁶⁸Ga. The unbounded ⁶⁸Ge was removed from the column with 20 mL of 0.05 M HCl. After 24 h, ⁶⁸Ga was eluted using 0.05 M HCl at a flow rate of 0.5 mL·min⁻¹. The final eluted ⁶⁸Ga-chloride was evaluated for metallic impurities, elution yield, breakthrough and fraction volume (Table 2). Based on encouraging results from the tests, we provided suggestions for future studies and the use of LC-TiO₂ as a ⁶⁸Ge/⁶⁸Ga generator column material.

Table 2. Performance of LC-TiO₂ adsorbent column.

Parameter	Previous Work [23]	This Work
Separation factor	1145	5439
Loaded activity (⁶⁸ Ge)	185 kBq	69 MBq
Eluent	0.01 M HCl	0.05 M HCl
⁶⁸ Ga elution yield (5 mL·min ⁻¹)	93.1%	93.2%
⁶⁸ Ga elution yield (gravity)	n/a	92%
Fraction volume	1.5 mL	1.0 mL
⁶⁸ Ge breakthrough (5 mL·min ⁻¹)	2.3×10^{-4}	1.6×10^{-4}
⁶⁸ Ge breakthrough (gravity)	n/a	3.1×10^{-4}
Metallic impurities	<100 ppb	<10 ppb

4. Materials and Methods

4.1. General

Low-molecular weight chitosan (MW 50,000–190,000 Da, cP 20–300) and P25 (titanium(IV) oxide, 21 nm) were obtained (Sigma-Aldrich, Saint Louis, MO, USA). For the labeling study, DOTA and NOTA chelator were obtained from MacroCyclic™. All optima grade acid solutions were purchased from Fisher Scientific (Waltham, MA, USA) and used without further purification. The ⁶⁸Ge-chloride source was obtained from Eckert & Ziegler (Berlin, Germany). ⁶⁸Ge/⁶⁸Ga generator (Eckert & Ziegler, Berlin, Germany) was used for a distribution coefficient of ⁶⁸Ga with 0.1 M HCl of an eluent. The activities of ⁶⁸Ge and ⁶⁸Ga were measured by a dose calibrator (Atomlab™, Biodex, New York, NY, USA). For measurement of ⁶⁸Ge breakthrough, a gamma counter (1480 WIZARD-3, Perkin Elmer, Trenton, NJ, USA) was used, and an in vivo study was conducted using a bench-top PET/X-ray system (Genesis 4, Perkin Elmer, Trenton, NJ, USA).

4.2. Preparation and Characterization of Chitosan-TiO₂ Adsorbent

The most common method for synthesizing chitosan-TiO₂ is mechanical stirring, followed by titanium metal trapped on the chitosan polymeric matrix (Figure 1). Solution I: 1.5 g of low molecule chitosan was dissolved in 5% acetic acid for 24 h. Solution II: 38.4 mL of absolute ethanol (99%) was mixed with 45 mL of TTIP dispersed in 6 mL of conc. HCl. TiO₂ metal powder (P25) (10 g) was added to the above mixture (solution II) and allowed to homogenize using an overhead stirrer for 16 h. The premixed solution was reacted with constant stirring for 2 h. After thorough homogenization of low molecular chitosan-TiO₂ (LC-TiO₂), the mixture was dropped into a 28% ammonia solution using a syringe pump (needle: 27G, flow rate: 7 mL·min⁻¹). The squashy LC-TiO₂ particles were washed and filtered by gravity with distilled water and dried for 12 h at 80 °C. Finally, prebuilt LC-TiO₂ was calcinated for 6 h at 450 °C using a muffle furnace (10 °C·min⁻¹).

4.3. Acid Resistance Study

The acid resistance of low-molecular weight chitosan-TiO₂ (LC-TiO₂) was estimated by focusing on the ⁶⁸Ga elution of extractants. The LC-TiO₂ adsorbent was placed in a 15 mL conical tube, followed by 5 mL of hydrochloric acid at various concentrations (0.01 M to 1.0 M). Then, physical stress was applied at 200 rpm for 1 to 48 h. After batch immersing experiments, the supernatant was collected and measured for metallic impurities by ICP-MS (7500 series, Agilent Technology, Inc., Santa Clara, CA, USA).

4.4. Distribution Coefficients (*K_d*)

The distribution coefficients of ⁶⁸Ge and ⁶⁸Ga with the LC-TiO₂ were carried out with various HCl concentrations (0.01 M to 1.0 M) at 37 °C for 3 h to determine their adsorption capacity. In brief, the ⁶⁸Ge/⁶⁸Ga equilibrated source (Eckert & Ziegler) was used for the *K_d* experiment.

The ⁶⁸Ge/⁶⁸Ga solutions (~37 kBq) were added to the LC-TiO₂ and shook constantly. After reaching the adsorption equilibrium, adsorbents were filtered out from equilibrium

solutions. The filtered solutions were determined instantly and after 24 h using a gamma counter. The calculation of the K_d was carried out as

$$K_d = \frac{(A_i - A_{eq})V}{mA_{eq}} \text{mL}\cdot\text{g}^{-1} \quad (1)$$

where K_d is the distribution coefficient ($\text{mL}\cdot\text{g}^{-1}$), A_i is initial aqueous phase activity of $^{68}\text{Ge}/^{68}\text{Ga}$ before equilibration, A_{eq} is final aqueous phase activity of $^{68}\text{Ge}/^{68}\text{Ga}$ after equilibration V is the volume (unit: mL) and m is the mass of adsorbent (grams).

4.5. Column Study

5 g of LC-TiO₂ was wet-packed into a 5 mL empty column (Eichrom) with 0.05 M HCl containing 74 MBq of $^{68}\text{Ge}/^{68}\text{Ga}$ solution. ^{68}Ga elution ability was tested under conditions of a flow rate of $5 \text{ mL}\cdot\text{min}^{-1}$ and gravity. The column was connected with a syringe pump using fluoropolymer resin tubing. After $^{68}\text{Ge}/^{68}\text{Ga}$ equilibrium, the column was rinsed with 20 mL of 0.01 M HCl to remove the unbound ^{68}Ge and then was left to stand for 24 h to demonstrate its performance. The column studies were repeated to confirm reproducibility.

4.6. ^{68}Ga Elution Profile and ^{68}Ge Breakthrough

Ten fractions of 1 mL volume were eluted at $0.5 \text{ mL}\cdot\text{min}^{-1}$ flow rate with a syringe pump for evaluating the elution yield of Ga. After 24 h, the remaining radioactivity was measured with a gamma counter to determine the breakthrough of ^{68}Ge .

4.7. Equilibrium Time of $^{68}\text{Ge}/^{68}\text{Ga}$

The synthesized LC-TiO₂ was completely soaked in 0.01 M HCl and then the supernatant was removed. ^{68}Ge stock solution (in 0.01 M HCl) (3.7 MBq) was added to the activated LC-TiO₂ adsorbent. The time to reach the $^{68}\text{Ge}/^{68}\text{Ga}$ equilibrium was evaluated by measuring the radioactivity over time for 50 h with a dose calibrator.

4.8. Radiolabeling and In Vivo Evaluation

Chelators (10 μM of DOTA and NOTA, respectively) were dissolved in sodium acetate (0.25 M, pH 4.5) solution. Chelator solutions were freshly prepared from stock solutions for each experiment. The ^{68}Ga -chloride solution ($\sim 59 \text{ MBq}\cdot\text{mL}^{-1}$) was purged with inert N₂ gas at 90 °C for 20 min (volume; $< 50 \mu\text{L}$). ^{68}Ga activity was added to the chelator solution (150 μL), and the reaction solutions were incubated at 100 °C and 25 °C, respectively. Samples of ^{68}Ga -DOTA and NOTA measured 12 min after labeling (Stationary phase: iTLC-SG, Mobile phase: 1:1/MeOH:10% NH₄OAc) are shown in Figure 7b,c.

For PET image scanning, balb/c mice were anesthetized with 2% isoflurane, and ^{68}Ga labeled compounds were injected by intravenous tail injection. PET images were acquired 5 and 30 min after injection.

5. Conclusions

In summary, we demonstrated that synthesized low molecular weight chitosan-TiO₂ can function as a column adsorbent for a $^{68}\text{Ge}/^{68}\text{Ga}$ generator. The fractions of the radionuclide generator need to be eluted and used immediately in the medical field, should not contain metallic impurities and must be used with high specific activity. Commercially available $^{68}\text{Ge}/^{68}\text{Ga}$ generators have a low labeling efficiency of ^{68}Ga with chelator agents due to metallic impurities in the final ^{68}Ga elution. The filter process of ^{68}Ga elution is generally conducted before the manufacture of ^{68}Ga -radiopharmaceuticals to avoid the effect of labeling yield by containing impure metals. We have developed a column adsorbent, which can overcome these limitations. The metallic impurities of the ^{68}Ga eluate were very low and had excellent $^{68}\text{Ge}/^{68}\text{Ga}$ adsorption and desorption capacities. Based on these results, we propose the use of LC-TiO₂ adsorbent for a $^{68}\text{Ge}/^{68}\text{Ga}$ generator system

with promising elution efficiency and stability and having the capability to provide a high purity of ^{68}Ga elution (>99.9%) with $10^{-4}\%$ of ^{68}Ge breakthrough.

Author Contributions: Conceptualization, J.-Y.L.; data curation, J.-Y.L.; formal analysis, J.-Y.L.; funding acquisition, J.-H.P.; investigation, J.-Y.L. and P.-S.C.; methodology, J.-Y.L.; project administration, J.-H.P.; validation, J.-H.P. and S.-D.Y.; visualization, J.-Y.L.; writing—original draft, J.-Y.L.; writing—review & editing, J.-H.P. and S.-D.Y. All authors have read and agreed to the published version of the manuscript.

Funding: This research was supported by the Nuclear R&D Program through the National Research Foundation of Korea, funded by the Ministry of Science, ICT, and Future Planning (2017M2A2A6A05016600 and 2021M2E7A1079112) and NTIS, Republic of Korea.

Institutional Review Board Statement: The study was conducted according to institutional animal care and use committee (IACUC) guidelines provided by Korea Atomic Energy Research Institute (IACUC number: KAERI 2021-010).

Informed Consent Statement: Not applicable.

Data Availability Statement: Not applicable.

Acknowledgments: This study was supported by a National Research Foundation Grant funded by the Korean Government (2017M2A2A6A05016600 and 2021M2E7A1079112) and NTIS, Republic of Korea.

Conflicts of Interest: The authors declare no conflict of interest. The funders had no role in the design of the study; in the collection, analyses, or interpretation of data; in the writing of the manuscript, or in the decision to publish the results.

Sample Availability: Samples of the compounds are not available from the authors.

References

1. Bé, M.M.; Schönfeld, E. Table de Radionucléide. 2012. Available online: http://www.nucleide.org/DDEP_WG/DDEPdata.htm (accessed on 9 April 2021).
2. Sanchez-Crespo, A. Comparison of Gallium-68 and Fluorine-18 imaging characteristics in positron emission tomography. *Appl. Radiat. Isot.* **2013**, *76*, 55–62. [[CrossRef](#)]
3. Banerjee, S.R.; Pomper, M.G. Clinical applications of Gallium-68. *Appl. Radiat. Isot.* **2013**, *76*, 2–13. [[CrossRef](#)] [[PubMed](#)]
4. Fani, M.; Andre, J.P.; Maecke, H.R. ^{68}Ga -PET: A powerful generator-based alternative to cyclotron-based PET radiopharmaceuticals. *Contrast Media Mol. Imaging* **2008**, *3*, 53–63. [[CrossRef](#)] [[PubMed](#)]
5. Velikyan, I. ^{68}Ga -based radiopharmaceuticals: Production and application relationship. *Molecules* **2015**, *20*, 12913–12943. [[CrossRef](#)] [[PubMed](#)]
6. Pauwels, E.; Cleeren, F.; Bormans, G.; Deroose, C.M. Somatostatin receptor PET ligands—the next generation for clinical practice. *Am. J. Nucl. Med. Mol. Imaging* **2018**, *8*, 311. [[PubMed](#)]
7. Ray Banerjee, S.; Chen, Z.; Pullambhatla, M.; Lisok, A.; Chen, J.; Mease, R.C.; Pomper, M.G. Preclinical comparative study of ^{68}Ga -labeled DOTA, NOTA, and HBED-CC chelated radiotracers for targeting PSMA. *Bioconjug. Chem.* **2016**, *27*, 1447–1455. [[CrossRef](#)]
8. Tsionou, M.I.; Knapp, C.E.; Foley, C.A.; Munteanu, C.R.; Cakebread, A.; Imberti, C.; Eykyn, T.R.; Young, J.D.; Paterson, B.M.; Blower, P.J. Comparison of macrocyclic and acyclic chelators for gallium-68 radiolabelling. *RSC Adv.* **2017**, *7*, 49586–49599. [[CrossRef](#)]
9. Rösch, F. Past, present and future of $^{68}\text{Ge}/^{68}\text{Ga}$ generators. *Appl. Radiat. Isot.* **2013**, *76*, 24–30. [[CrossRef](#)]
10. Chakravarty, R.; Chakraborty, S.; Ram, R.; Vatsa, R.; Bhusari, P.; Shukla, J.; Mittal, B.; Dash, A. Detailed evaluation of different $^{68}\text{Ge}/^{68}\text{Ga}$ generators: An attempt toward achieving efficient ^{68}Ga radiopharmacy. *J. Label. Compd. Radiopharm.* **2016**, *59*, 87–94. [[CrossRef](#)]
11. Kumar, K.Y.; Muralidhara, H.; Nayaka, Y.A.; Balasubramanyam, J.; Hanumanthappa, H. Low-cost synthesis of metal oxide nanoparticles and their application in adsorption of commercial dye and heavy metal ion in aqueous solution. *Powder Technol.* **2013**, *246*, 125–136. [[CrossRef](#)]
12. Mironyuk, I.; Tatarchuk, T.; Vasylyeva, H.; Naushad, M.; Mykytyn, I. Adsorption of Sr (II) cations onto phosphated mesoporous titanium dioxide: Mechanism, isotherm and kinetics studies. *J. Environ. Chem. Eng.* **2019**, *7*, 103430. [[CrossRef](#)]
13. Mainier, F.B.; Monteiro, L.P.; Tavares, S.S.; Leta, F.R.; Pardal, J.M. Evaluation of titanium in hydrochloric acid solutions containing corrosion inhibitors. *IOSR J. Mech. Civ. Eng.* **2003**, *10*, 66–69. [[CrossRef](#)]
14. de Blois, E.; Chan, H.S.; Naidoo, C.; Prince, D.; Krenning, E.P.; Breeman, W.A. Characteristics of SnO_2 -based $^{68}\text{Ge}/^{68}\text{Ga}$ generator and aspects of radiolabelling DOTA-peptides. *Appl. Radiat. Isot.* **2011**, *69*, 308–315. [[CrossRef](#)] [[PubMed](#)]

15. Egamediev, S.; Khujaev, S.; Mamatkazina, A. Influence of preliminary treatment of aluminum oxide on the separation of ^{68}Ge - ^{68}Ga radionuclide chain. *J. Radioanal. Nucl. Chem.* **2000**, *246*, 593–596. [[CrossRef](#)]
16. Lin, M.; Ranganathan, D.; Mori, T.; Hagooley, A.; Rossin, R.; Welch, M.J.; Lapi, S.E. Long-term evaluation of TiO_2 -based $^{68}\text{Ge}/^{68}\text{Ga}$ generators and optimized automation of [^{68}Ga] DOTATOC radiosynthesis. *Appl. Radiat. Isot.* **2012**, *70*, 2539–2544. [[CrossRef](#)] [[PubMed](#)]
17. Anaya-Esparza, L.M.; Ruvalcaba-Gómez, J.M.; Maytorena-Verdugo, C.I.; González-Silva, N.; Romero-Toledo, R.; Aguilera-Aguirre, S.; Pérez-Larios, A. Chitosan- TiO_2 : A Versatile Hybrid Composite. *Materials* **2020**, *13*, 811. [[CrossRef](#)] [[PubMed](#)]
18. Deveci, I.; Doğaç, Y.I.; Teke, M.; Mercimek, B. Synthesis and characterization of chitosan/ TiO_2 composite beads for improving stability of porcine pancreatic lipase. *Appl. Biochem. Biotechnol.* **2015**, *175*, 1052–1068. [[CrossRef](#)]
19. Jiang, R.; Zhu, H.-Y.; Chen, H.-H.; Yao, J.; Fu, Y.-Q.; Zhang, Z.-Y.; Xu, Y.-M. Effect of calcination temperature on physical parameters and photocatalytic activity of mesoporous titania spheres using chitosan/poly (vinyl alcohol) hydrogel beads as a template. *Appl. Surf. Sci.* **2014**, *319*, 189–196. [[CrossRef](#)]
20. Kravanja, G.; Primožič, M.; Knez, Ž.; Leitgeb, M. Chitosan-based (Nano) materials for novel biomedical applications. *Molecules* **2019**, *24*, 1960. [[CrossRef](#)]
21. Franca, E.F.; Freitas, L.C.; Lins, R.D. Chitosan molecular structure as a function of N-acetylation. *Biopolymers* **2011**, *95*, 448–460. [[CrossRef](#)]
22. Rashid, S.; Shen, C.; Yang, J.; Liu, J.; Li, J. Preparation and properties of chitosan–metal complex: Some factors influencing the adsorption capacity for dyes in aqueous solution. *J. Environ. Sci.* **2018**, *66*, 301–309. [[CrossRef](#)]
23. Upadhyay, U.; Sreedhar, I.; Singh, S.A.; Patel, C.M.; Anitha, K. Recent advances in heavy metal removal by chitosan based adsorbents. *Carbohydr. Polym.* **2020**, *251*, 117000. [[CrossRef](#)] [[PubMed](#)]
24. Vyas, C.K.; Lee, J.Y.; Hur, M.G.; Yang, S.D.; Kong, Y.B.; Lee, E.J.; Park, J.H. Chitosan- TiO_2 composite: A potential $^{68}\text{Ge}/^{68}\text{Ga}$ generator column material. *Appl. Radiat. Isot.* **2019**, *149*, 206–213. [[CrossRef](#)]
25. Luong, H.T.; Liu, J. Flotation separation of gallium from aqueous solution—effects of chemical speciation and solubility. *Sep. Purif. Technol.* **2014**, *132*, 115–119. [[CrossRef](#)]
26. Bacsá, R.R.; Grätzel, M. Rutile formation in hydrothermally crystallized nanosized titania. *J. Am. Ceram. Soc.* **1996**, *79*, 2185–2188. [[CrossRef](#)]